Real-time Attitude Estimation Techniques Applied to a Four Rotor Helicopter

Matthew G. Earl and Raffaello D'Andrea

Abstract— We use a decomposition approach to develop a real time filter that estimates the attitude of a small four rotor helicopter. The filter uses measurements from a three axis gyro system and an off-board computer vision system. We have implemented the filter on the real system to demonstrate its effectiveness.

I. INTRODUCTION

Autonomous flight continues to be an intense field of research because of the numerous practical uses for such vehicles. Many of the most useful applications for this technology include performing dull, dirty, and dangerous tasks. Some examples include exploration, scientific data collection, search and rescue missions, and communications.

We have built a team of four rotor helicopters for research on multi-vehicle cooperative control such as vehicle based antenna arrays [1]. In this paper, we focus on attitude estimation for a single helicopter. The helicopter is instrumented with rate gyros that measure angular velocity about a body fixed set of axes at a high rate. We use an off-board vision system to measures helicopter attitude at a low rate. The goal is to develop an estimator to fuse the two sources of attitude information obtaining an optimal estimate of the helicopter's attitude. The full estimation problem is nonlinear, highly coupled, and very difficult to solve in real time. Here, we describe a decomposition approach for real time estimation and apply the approach to estimate the orientation of the four rotor helicopter.

In Section II we describe the four rotor helicopter and the setup we use to control it. In Section III we give an overview of our decomposition approach. In Sections IV and V we describe the vision and gyro measurement transformations that allow the estimation problem to be decoupled. In Section VI we describe the Kalman Filter for the optimal estimate of vehicle orientation. Finally, in Section VII we show the results of our approach applied to the four rotor helicopter.

II. SETUP

The flying vehicle we have built is a four rotor helicopter depicted in Figure 1. The propellers, mounted at the corners of a carbon-fiber rod structure, are driven by four geared electric motors. LEDs are mounted at the corners for

M. Earl is with the Department of Theoretical and Applied Mechanics, Cornell University, Ithaca, New York mge1@cornell.edu

R. D'Andrea is with the Department Mechanical and Aerospace Engineering, Cornell University, Ithaca, New York rd28@cornell.edu
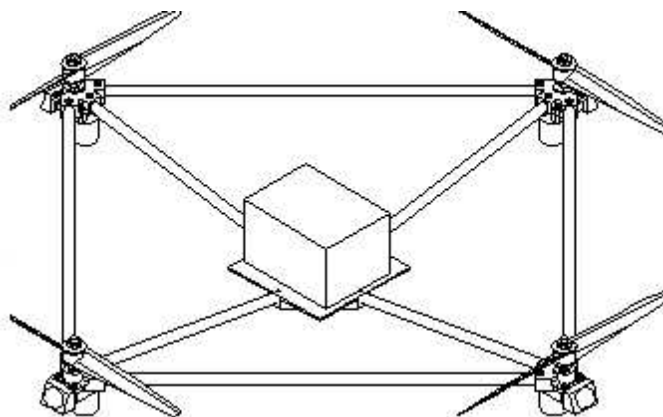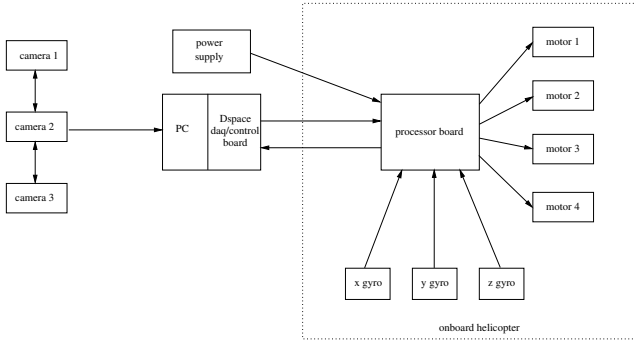
Fig. 1.   Assembly diagram of the four rotor helicopter.

attitude and position sensing by the vision system. The on-board electronics package is mounted at the center of the structure.

Figure 2 shows a block diagram of the interconnections between components of the system. The rate gyros, located in the on-board electronics package, measure angular velocity about a body fixed set of axes. The gyro data is sent to an on-board processor then forwarded to an off-board PC, which calculates the control inputs for the vehicle. The on-board processor receives commands from the off-board PC and forwards them to the motors. Communications between on-board and off-board processors occur over a wire tether hanging from the helicopter. The tether also supplies power to the helicopter. In Figure 2 the connections that pass through the dotted box represent the tethered link.

The vision system consists of three cameras mounted orthogonally to the test section. The cameras are synchronized and send frames to the off-board control PC at a rate of ten frames per second.

The off-board control PC receives measurements from the vision system and the gyros, processes these data, and then sends appropriate control commands to the helicopter to achieve a desired objective.

III. THE DECOMPOSITION

Given vision measurements of the LEDs with respect to a fixed coordinate system and gyro measurements of angular velocity with respect to a set of body axes attached to the helicopter (defined by the orientation of the gyros on the electronic board), our objective is to determine an optimal estimate of the helicopter's attitude. We use the Euler angles

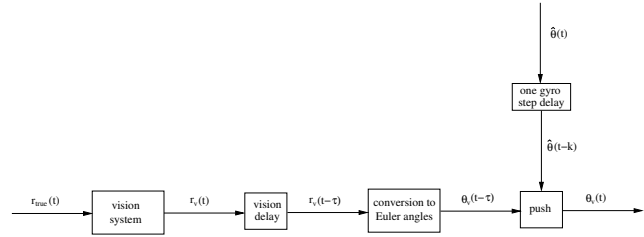Fig. 2. Diagram of the interconnections between components of the system.

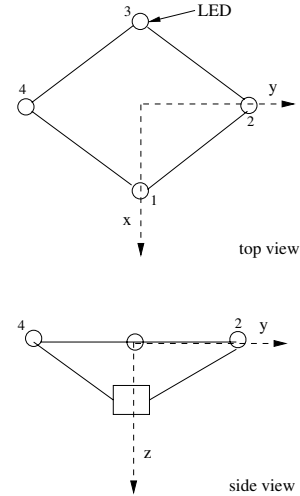Fig. 3. Diagram of component 1: vision measurement transformation and push ahead.

Fig. 4. The body axis coordinate systems attached to the helicopter. For small angle changes: ψ is a rotation about the x axis, and θ is a rotation about the y axis, ϕ is a rotation about the z axis.

$\Theta = (\psi, \theta, \phi)$ to describe the attitude of the helicopter.

This problem is difficult because the helicopter equations of motion are nonlinear, the vision and gyro measurement equations are nonlinear and coupled, and the vision measurements significantly delayed due to latency in the system.

To make the problem manageable for real time estimation we decompose it into three components:

1) *Vision measurement transformation and push ahead.* At each vision step the coordinates of the four LEDs are measured. We convert these measurements into an estimate of the Euler angles by first solving a nonlinear least squares problem. Then, using previous Euler angle estimates, we push the computed Euler angles ahead in time to counteract latency.

2) *Gyro data transformation.* At each gyro step we transform the gyro measurements of body axis angular velocity into Euler rates. This is done using the standard kinematic equations. This is an approximate approach because we use Euler angle estimates from the previous gyro step in place of the current Euler angles. This approximation is reasonable because the gyro step is very fast (300Hz),

3) *Kalman Filter.* Using the two different sources of attitude computed in components 1 and 2, we develop Kalman Filters that compute an optimal estimate of each Euler angle. The filters are independent because components 1 and 2 decouple the problem.

This decomposition makes the problem tractable, greatly decreases the computation requirements, and works well in practice as we show next.

IV. VISION MEASUREMENT TRANSFORMATION AND PUSH AHEAD

This step is depicted in Figure 3. First, we describe the conversion to Euler angles box, which uses a nonlinear least squares method to estimate the Euler angles from vision measurements. Then, we describe the push ahead box.

A. Conversion to Euler angles

There are four LEDs attached to the helicopter as depicted in Figures 1 and 4. The vision system measures the coordinates of each LED with respect to a fixed coordinate system with origin defined by the center of mass of the helicopter. The orientation of this coordinate system is taken to be the initial orientation of the helicopter. We denote the normalized coordinates of the ith LED with respect to the vision system's fixed coordinate system as,

$$r_i(t) = (x_i(t), y_i(t), z_i(t)). \tag{1}$$

Assuming that the center of mass is located on the plane that contains the four LEDs we have

$$\begin{aligned} r_1(0) &= (1, 0, 0) \\ r_2(0) &= (0, 1, 0) \\ r_3(0) &= (-1, 0, 0) \\ r_4(0) &= (0, -1, 0). \end{aligned} \tag{2}$$

The coordinates of the ith LED at time t can be expressed as a rotation of the coordinate vector at time zero, namely

$$r_i(t) = A(t)r_i(0), \tag{3}$$

where the rotation matrix $A(t)$ is a function of the Euler angles $\theta(t)$, $\phi(t)$, and $\psi(t)$ [4].

The coordinates for LEDs 1 and 3 are given by

$$r_1(t) = A(t)r_1(0)$$
$$r_3(t) = A(t)r_3(0). \tag{4}$$

Subtracting these two equations and substituting values from equation (2) yields,

$$r_1(t) - r_3(t) = 2A(t) \begin{bmatrix} 1 \\ 0 \\ 0 \end{bmatrix}. \tag{5}$$

Similarly, for LEDs 2 and 4,

$$r_2(t) - r_4(t) = 2A(t) \begin{bmatrix} 0 \\ 1 \\ 0 \end{bmatrix}. \tag{6}$$

Combining these two equations we get the measurement equation

$$\frac{1}{2} \begin{bmatrix} r_1(t) - r_3(t) \\ r_2(t) - r_4(t) \end{bmatrix} = \begin{bmatrix} \cos(\theta)\cos(\phi) \\ \cos(\theta)\sin(\phi) \\ -\sin(\theta) \\ \sin(\psi)\sin(\theta)\cos(\phi) - \cos(\phi)\sin(\phi) \\ \sin(\psi)\sin(\theta)\sin(\phi) + \cos(\psi)\cos(\phi) \\ \cos(\theta)\cos(\phi) \end{bmatrix}. \tag{7}$$

We can write this in a more compact form by letting the right hand side equal $h(\Theta)$ where $\Theta = (\psi, \theta, \phi)$. The left hand side represents the measurements denoted by y. The measurements are corrupted by noise v, modeled as zero-mean white Gaussian noise $v \sim N(0, I)$. Therefore, the measurement equation can be written as

$$y(t) = h(\Theta(t)) + v(t), \tag{8}$$

which is a set of six equations in three unknowns (the system is over-determined).

To obtain an estimate for the Euler angles from equation (8) we calculate the maximum likelihood estimate by minimizing the cost

$$J = \frac{1}{2}v^T v = \frac{1}{2}(y - h(\Theta))^T (y - h(\Theta)). \tag{9}$$

Differentiating the cost with respect to the Euler angles we get

$$\frac{\partial J}{\partial \Theta} = -(y - h(\Theta))^T D_h(\Theta), \tag{10}$$

where D_h is the Jacobian matrix of h with respect to Θ. A necessary condition for a minimum is that $\frac{\partial J}{\partial \Theta} = 0$. Therefore, the following equation must be satisfied at the minimum,

$$f(\Theta) = D_h(\Theta)^T (y - h(\Theta)) = 0. \tag{11}$$

These are three equations in three unknowns that we solve numerically using the Gauss-Newton method.

We are looking for the zeros of $f(\Theta)$. First, we make a guess Θ_g and linearize about the guess by letting $\Theta = \Theta_g + \Delta\Theta$. We write $f(\Theta)$ as the expansion

$$f(\Theta_g + \Delta\Theta) = f(\Theta_g) + Df(\Theta_g)\Delta\Theta + O(\Delta\Theta^2), \tag{12}$$

where $Df(\Theta_g)$ is the Jacobian matrix of $f(\Theta)$ evaluated at Θ_g given by

$$Df(\Theta_g) = -DDh(\Theta_g)^T (y - h(\Theta_g)) + Dh(\Theta_g)^T Dh(\Theta_g). \tag{13}$$

Now we solve for the zeros of f neglecting the higher order terms in $\Delta\Theta$,

$$f(\Theta_g) + Df(\Theta_g)\Delta\Theta = 0, \tag{14}$$

and we solve for $\Delta\Theta$ to get

$$\Delta\Theta = -Df(\Theta_g)^{-1}f(\Theta_g). \tag{15}$$

We repeat the process with a new guess given by

$$\Theta_g^{(new)} = \Theta_g + \Delta\Theta \tag{16}$$

and continue iteratively until $\Delta\Theta \to 0$.

We take Θ calculated at the previous vision step as the initial guess Θ_g. Because the vision updates at 10Hz, we expect the first term in equation (13), which is a second order differential term, to be small. Hence,

$$Df(\Theta_g) \approx Dh(\Theta_g)^T Dh(\Theta_g), \tag{17}$$

and substituting equations (11) and (17) into equation (15) we get,

$$\Delta\Theta = M(\Theta_g)(y - h(\Theta_g)), \tag{18}$$

where $M(\Theta_g) = -\left[Dh(\Theta_g)^T Dh(\Theta_g)\right]^{-1} Dh(\Theta_g)^T$.

B. The push ahead

Using the transformation described above we can determine the Euler angles $\Theta_v(t - \tau) = (\theta_v(t - \tau), \phi_v(t - \tau), \psi_v(t - \tau))$. These angles are time delayed by $\tau = 0.2$ seconds, where τ is given by the latency in the vision system. Now the problem is decoupled and we can consider the push ahead of each Euler angle independently. Here we consider $\theta(t)$, but the procedure is the same for each of the Euler angles.

Consider the equation

$$\theta(t) = \theta(t - \tau) + \theta(t) - \theta(t - \tau). \tag{19}$$

We can use this equation to push the vision measurement ahead in time by using the optimal estimates of θ for the last two terms,

$$\theta_v(t) \approx \theta_v(t - \tau) + \hat{\theta}(t) - \hat{\theta}(t - \tau). \tag{20}$$

Because we do not have access to $\hat{\theta}(t)$, we use the estimate from the last gyro step $\hat{\theta}(t - k)$ where $k = 1/300$ seconds is small so the approximation is valid. This yields,

$$\theta_v(t) \approx \theta_v(t - \tau) + \hat{\theta}(t - k) - \hat{\theta}(t - \tau). \tag{21}$$

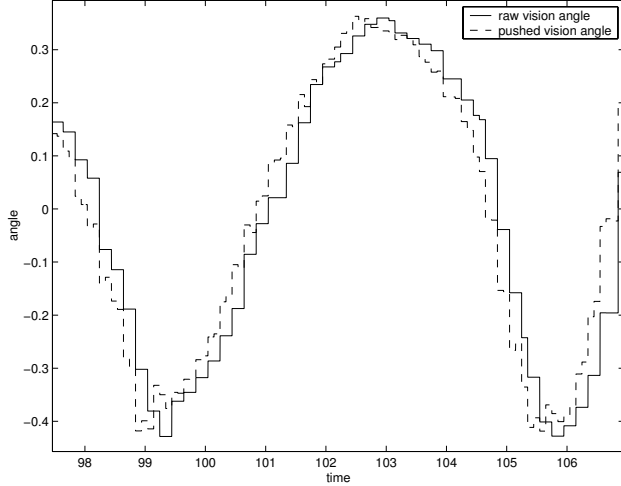Figure 5 shows results of the push ahead as the helicopter oscillates.

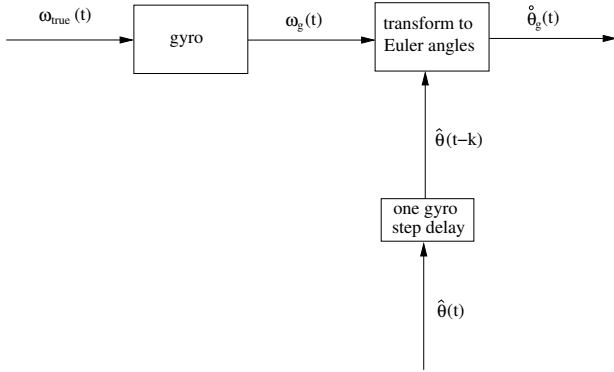Fig. 5. The push ahead in θ_v as the helicopter oscillates.

Fig. 6. Diagram of component 2: gyro measurement transformation.

V. GYRO MEASUREMENT TRANSFORMATION

In this component, we transform the gyro body axis angular velocity measurements $\omega_g = (\omega_g^{(x)}, \omega_g^{(y)}, \omega_g^{(z)})$ into Euler rates $\dot{\Theta}_g = (\dot{\psi}_g, \dot{\theta}_g, \dot{\phi}_g)$ as depicted in the block diagram in Figure 6. The Euler rates can be written in terms of the Euler angles and the body axis angular velocity [4], namely

$$
\begin{aligned}
\dot{\psi} &= \omega_x + \omega_y \sin(\psi)\tan(\theta) + \omega_z \cos(\psi)\tan(\theta) \\
\dot{\theta} &= \omega_y \cos(\psi) - \omega_z \sin(\psi) \\
\dot{\phi} &= \omega_y \frac{\sin(\psi)}{\cos(\theta)} + \omega_z \frac{\cos(\psi)}{\cos(\theta)}.
\end{aligned} \tag{22}
$$

We have a measurement of the angular velocity from the gyro system, but we do not have a direct measurement of $\Theta(t)$. For $\Theta(t)$, we use the optimal estimate of the Euler angles at the previous gyro step $\hat{\Theta}(t-k)$. Therefore, an estimate of the current Euler rates $\dot{\Theta}_g(t)$ is given by

$$
\begin{aligned}
\dot{\psi}_g(t) &\approx \omega_g^{(x)} + \omega_g^{(y)} \sin(\hat{\psi}(t-k))\tan(\hat{\theta}(t-k)) \\
&\quad + \omega_g^{(z)} \cos(\hat{\psi}(t-k))\tan(\hat{\theta}(t-k)) \\
\dot{\theta}_g(t) &\approx \omega_g^{(y)} \cos(\hat{\psi}(t-k)) - \omega_g^{(z)} \sin(\hat{\psi}(t-k))
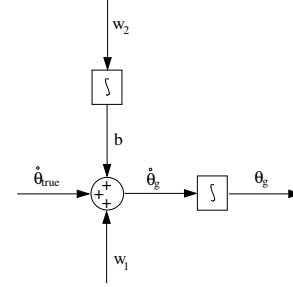\end{aligned}
$$

Fig. 7. Block diagram of the decoupled single axis gyro model.

$$
\dot{\phi}_g(t) \approx \omega_g^{(y)} \frac{\sin(\hat{\psi}(t-k))}{\cos(\hat{\theta}(t-k))} + \omega_g^{(z)} \frac{\cos(\hat{\psi}(t-k))}{\cos(\hat{\theta}(t-k))}. \tag{23}
$$

This approximation works well in practice because the gyro data rate is very fast (300Hz).

VI. THE KALMAN FILTER

While the gyros provide very good high frequency information, a small bias in the rate measurement will result in unbounded drift in the orientation angle calculated by integrating the rate measurement. To circumvent this limitation, we have introduced an external vision system as another source of orientation information. The vision measurements are very good on average (good low frequency information). However, they are not accurate at high frequencies because the data rate is low. The goal of this Kalman Filter is to optimally fuse the gyro and vision information so that the resulting orientation estimate has the high frequency qualities of the gyro measurement and the low frequency qualities of the vision measurement.

An important aspect of implementation is the total state space vs. error state space formulation of the filtering problem (also known as direct vs. indirect filtering) [6]. In the total state space formulation the model for the filter is a set of dynamic equations governing the state of the system. The inputs to the filter would include both gyro and vision measurements. In the error state formulation the Kalman Filter estimates the errors in the gyro information using the difference between gyro and vision data as the measurements. Because the gyros follow the high frequency dynamics very accurately, there is no need to model them explicitly. We use the error state formulation, which is normally used for externally aided inertial navigation systems because of its many benefits including relative simplicity and reduced computation requirements.

The gyro is modeled as a continuous system since the data rate is very high (300Hz). The model, depicted in Figure 7, is an integrator of angular velocity $\dot{\theta}_{true}$ corrupted by white Gaussian noise w_1 and bias b. The bias is modeled as a random walk, i.e., an integrator driven by zero mean white Gaussian noise w_2. The governing equations of the

gyro model are

$$\dot{\theta}_g(t) = \dot{\theta}_{true}(t) + b(t) + w_1(t)$$
$$\dot{b}(t) = w_2(t) \tag{24}$$

where $E\{w_1(t)\} = 0$, $E\{w_2(t)\} = 0$, $E\{w_1(t)w_1(t+\tau)\} = Q_1\delta(\tau)$, and $E\{w_2(t)w_2(t+\tau)\} = Q_2\delta(\tau)$.

The vision system is modeled as a discrete time system since the data rate is relatively low (10Hz). The model is taken as the angle θ_{true} corrupted by zero mean white Gaussian noise v of strength R, and is given by

$$\theta_v(t_i) = \theta_{true}(t_i) - v(t_i), \tag{25}$$

where $E\{v(t_i)\} = 0$ and $E\{v(t_i)v(t_i)\} = R$.

The error state for the filter is the gyro error

$$\delta\theta(t) = \theta_g(t) - \theta_{true}(t). \tag{26}$$

The states for our filter are the gyro error $\delta\theta$ and the gyro bias b. They are governed by

$$\dot{\delta\theta}(t) = b(t) + w_1(t) \tag{27}$$
$$\dot{b}(t) = w_2(t), \tag{28}$$

or in matrix form, $\dot{x}(t) = Fx(t) + Gw(t)$, we have

$$\begin{bmatrix} \dot{\delta\theta}(t) \\ \dot{b}(t) \end{bmatrix} = \begin{bmatrix} 0 & 1 \\ 0 & 0 \end{bmatrix} \begin{bmatrix} \delta\theta(t) \\ b(t) \end{bmatrix} + \begin{bmatrix} 1 & 0 \\ 0 & 1 \end{bmatrix} \begin{bmatrix} w_1(t) \\ w_2(t) \end{bmatrix}. \tag{29}$$

The measurement for the filter (input to the filter) is the difference between the gyro angle and the vision angle in discrete time

$$z(t_i) = \theta_g(t_i) - \theta_v(t_i)$$
$$= [\theta_{true}(t_i) + \delta\theta(t_i)] - [\theta_{true}(t_i) - v(t_i)]$$
$$= \delta\theta(t_i) + v(t_i). \tag{30}$$

In matrix form, $z(t) = Hx(t) + v(t)$, the measurement equation is given by

$$z(t_i) = \begin{bmatrix} 1 & 0 \end{bmatrix} \begin{bmatrix} \delta\theta(t_i) \\ b(t_i) \end{bmatrix} + v(t_i). \tag{31}$$

The initial condition is modeled as a Gaussian random variable with mean

$$E\{x(t_o)\} = \hat{x}_o = \begin{bmatrix} 0 \\ b_o \end{bmatrix}, \tag{32}$$

and covariance

$$P_o = \begin{bmatrix} \sigma_\theta^2 & 0 \\ 0 & \sigma_b^2 \end{bmatrix}. \tag{33}$$

The variance in uncertainty in knowledge of initial angle and bias is represented by the diagonal terms σ_θ^2 and σ_b^2, respectively. There is no initial cross correlation between angle and bias as represented by zeros off the diagonal in P_o.

The Kalman Filter is composed of two stages: propagation and update. To incorporate new measurement $z(t_i)$ into the estimate of the state, first, the state estimate at t_{i-1}, namely $\hat{x}(t_{i-1})$, must be propagated from time t_{i-1}^+

to time t_i^- using the dynamic equation without noise terms, $\dot{x}(t) = Fx(t)$, given by

$$\begin{bmatrix} \dot{\delta\theta}(t) \\ \dot{b}(t) \end{bmatrix} = \begin{bmatrix} 0 & 1 \\ 0 & 0 \end{bmatrix} \begin{bmatrix} \delta\theta(t) \\ b(t) \end{bmatrix}. \tag{34}$$

The solution to the general propagation equation is

$$\hat{x}(t_i^-) = e^{F(t_i - t_{i-1})}\hat{x}(t_{i-1}^+), \tag{35}$$

and the solution to the propagation equation for our case is

$$\begin{bmatrix} \hat{\delta\theta}(t_i^-) \\ \hat{b}(t_i^-) \end{bmatrix} = \begin{bmatrix} 1 & t_i - t_{i-1} \\ 0 & 1 \end{bmatrix} \begin{bmatrix} \hat{\delta\theta}(t_{i-1}^+) \\ \hat{b}(t_{i-1}^+) \end{bmatrix}. \tag{36}$$

The covariance is propagated using the following matrix differential equation [6], [3]

$$\dot{P}(t) = FP(t) + P(t)F^T + GQG^T. \tag{37}$$

Now that we have $\hat{x}(t_i^-)$ and $P(t_i^-)$ we can incorporate the new measurement $z(t_i)$ into the estimate. To do this we use the update equations [6], [3]

$$K(t_i) = P(t_i)H^T \left[HP(t_i^-)H^T + R \right]^{-1}$$
$$\hat{x}(t_i^+) = \hat{x}(t_i^-) + K(t_i) \left[z(t_i) - H\hat{x}(t_i^-) \right]$$
$$P(t_i^+) = P(t_i^-) - K(t_i)HP(t_i^-). \tag{38}$$

For our case the update equations are

$$\begin{bmatrix} \hat{\delta\theta}(t_i^+) \\ \hat{b}(t_i^+) \end{bmatrix} = \begin{bmatrix} \hat{\delta\theta}(t_i^-) \\ \hat{b}(t_i^-) \end{bmatrix} + \begin{bmatrix} K_1(t_i) \\ K_2(t_i) \end{bmatrix} \left[z(t_i) - \hat{\delta\theta}(t_i^-) \right]. \tag{39}$$

In between measurements the optimal estimates of orientation angle and gyro bias are governed by

$$\dot{\hat{\theta}}(t) = \dot{\theta}_g(t) - \hat{b}(t)$$
$$\dot{\hat{b}}(t) = 0. \tag{40}$$

When a measurement is available the orientation angle and the gyro are updated. The update equations are

$$\hat{\theta}(t_i^+) = \theta_g(t_i) - \hat{\delta\theta}(t_i^+)$$
$$= \hat{\theta}(t_i^-) + K_1(t_i) \left[\hat{\theta}(t_i^-) - \theta_v(t_i) \right]$$
$$\hat{b}(t_i^+) = \hat{b}(t_i^-) + K_2(t_i) \left[\hat{\theta}(t_i^-) - \theta_v(t_i) \right]. \tag{41}$$

This is illustrated in Figure 8. We take the time varying matrix $K(t_i) = [K_1(t_i), K_2(t_i)]^T$ to be constant since it settles down to steady state quickly.

VII. RESULTS

We have implemented our three component decomposition approach on the actual system using Simulink [5] to create the code and dSpace [2] to implement it on the control computer processor. The approach works well in practice as depicted in the plots in Figures 9 and 10. Figure 9 shows the gyro measurements, the vision measurements, and the optimal estimate as the helicopter oscillates. Figure 10 shows the measurements and the optimal estimate when the helicopter is stationary.
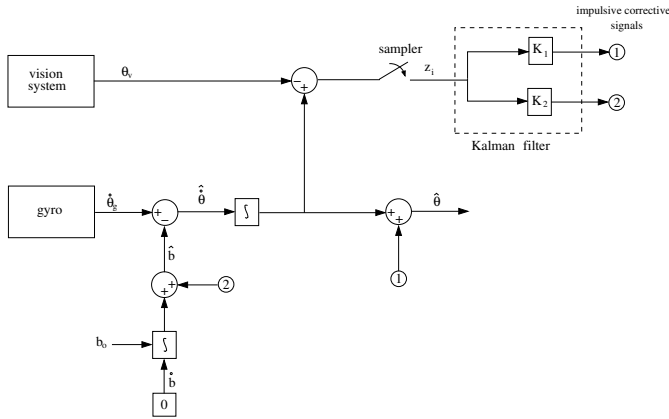
Fig. 8. Diagram of step 3: the Kalman Filter.

The estimated angle has the best qualities of both the vision measurement (low frequency) and the gyro measurement (high frequency). The negative qualities of drift in the gyro measurements and the low data rate and latency in the vision measurements are eliminated in the optimal estimate.

ACKNOWLEDGMENT

We thank the students that helped design and build the helicopter: Sean Breheny, Owen Fong, S. Leard Huggins IV, and Alexandre Saverin.

REFERENCES

[1] S. H. Breheny, R. D'Andrea, and J. C. Miller, "Using airborne vehicle-based antenna arrays to improve communications with UAV clusters," *Proceedings. 42nd IEEE Conference on Decision and Control*, Dec. 2003, pp. 4158–4162.
[2] dSpace. http://www.dspaceinc.com
[3] A. Gelb, *Applied Optimal Estimation*. Massachusetts: MIT press, 1974.
[4] H. Goldstein, *Classical Mechanics*. 2nd ed. Massachusetts: Addison-Wesley, 1980.
[5] Matlab. http://www.mathworks.com
[6] P. S. Maybeck, *Stochastic Models, Estimation, and Control Volume 1*. Arlington, VA: Navtech Book, 1994.
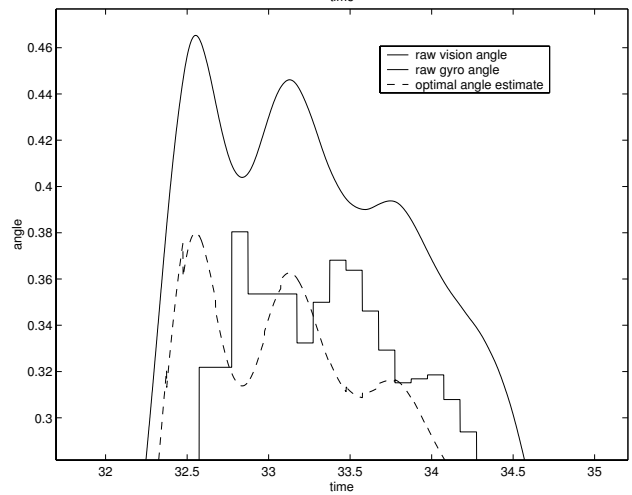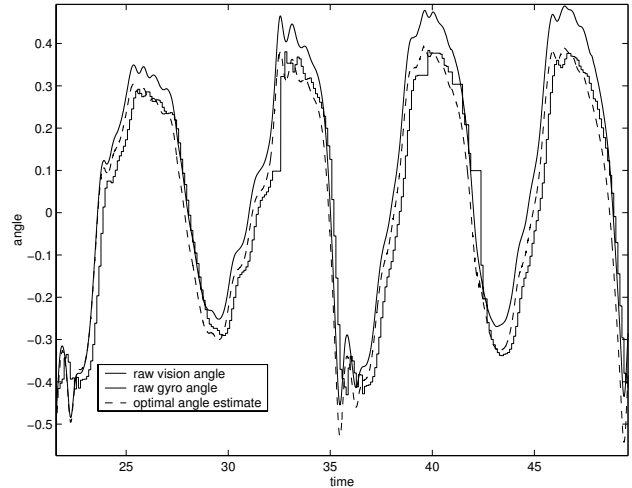
Fig. 9. The raw gyro angle (solid line), the raw vision angle (solid piecewise constant line), and the optimal estimate (dashed line) of helicopter Euler angle θ as the helicopter oscillates. The second figure is a magnification of the first figure in time window $[32, 35]$. The optimal estimate has the best qualities of the vision measurement (low frequency behavior) and the gyro measurement (high frequency behavior).
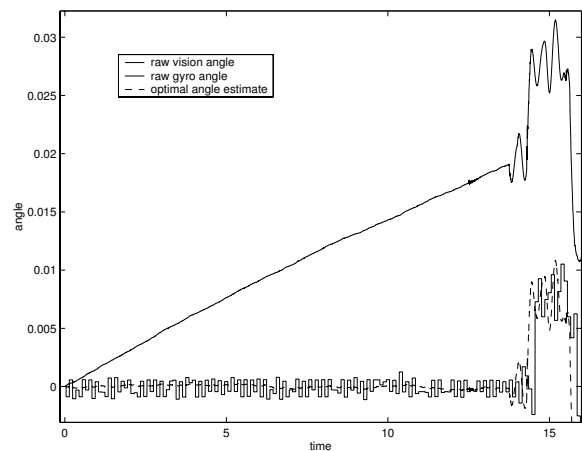

Fig. 10. Euler angle measurements and estimate as in Figure 9. The helicopter is still for the first 14 seconds before it oscillates. Notice that the raw gyro angle drifts as the bias from the gyro rate measurement is integrated.